LUNAR REGOLITH BRECCIA METEORITE NORTHWEST AFRICA 8783: CLAST DIVERSITY WITH IMPLICATIONS FOR BOMBARDMENT HISTORY AND CRUSTAL EVOLUTION. A. L. Fagan[1], K. H. Joy[2], M. Hall[1], E. M. Recchuiti[1], C. Utterback[1], and S. E. Roberts[3], [1]Geosciences and Natural Resources Dept., Western Carolina University, Cullowhee, NC 28723, USA (alfagan@wcu.edu), [2] School of Earth and Environmental Sciences, University of Manchester, Manchester, M13 9PL, UK, [3] Dept. of Earth and Planetary Sciences, Univ. of Tennessee, Knoxville TN 37996, USA.

Introduction: Lunar regolith breccias hold a wealth of information that address several large questions of the evolution and the bombardment history of the Moon such as the temporal change in impactor populations [1-3]. Regolith breccias contain abundant solar wind input, glass spherules, and agglutinates, thus preserving the history of impact events on the lunar surface. Diverse, isolated mineral grains and lithic clasts also represent a large area sampled as a result of regolith gardening [e.g., 4]. Therefore, these samples can reveal more information about the composition, diversity, and temporal changes of lunar surface materials, which are key areas of investigation for understanding the evolution of the Moon and inner solar system [e.g., 5-7].

In this study, we examine 6 lithic clasts (Fig. 1) from two thin-sections of lunar regolith breccia meteorite Northwest Africa (NWA) 8783 to address the compositional diversity and bombardment history of the Moon through mineral geochemistry and geochronology.

NWA8783 Description: NWA 8783 is paired with NWA 8455, NWA8609, NWA 8667, and NWA 10130, and has similar bulk composition (e.g., Sm, Sc, Th) to the Apollo 16 regolith [8-9]. The meteorite contains a range of isolated mineral clasts as well as lithic clasts set in a dark, fine-grained matrix that is cross-cut by yellow impact glass veins. This study focuses on two main types of clasts: a large (1.75 x 4.5 mm) impact melt clast (Fig. 1d) and 5 endogenous igneous clasts. Clast 1 (Fig. 1a) is predominantly composed of elongated enstatite and augite crystals as well as a single, small (<20 μm) anhedral olivine and ilmenite poikilitically enclosed by an enstatite. Clasts 2 (Fig. 1b) and 3 are composed of pyroxene subophitically to ophitically enclosing plagioclase with intergranular olivine. Clasts 5 and 6 (Fig. 1c) have granulitic textures dominated by plagioclase and olivine, with Clast 5 also having pyroxene. Clast 7 (Fig. 1d), a recrystallized impact melt, displays a range of textures including sub-ophitic to ophitic, intersertal, and intergranular, and is dominated by plagioclase laths with pyroxene, olivine, and K-rich interstitial glass.

Methods: *Electron Probe Microanalysis (EPMA):* Major and minor elemental abundances of plagioclase, olivine, pyroxene, ilmenite, and glass were characterized using electron probe microanalysis (EPMA) via the Cameca SX 100 at the Univ. of Tennessee; instrument settings were: 15 kV, 30nA, and on-peak count times of 30 sec; natural and synthetic materials were used as standards reference material.

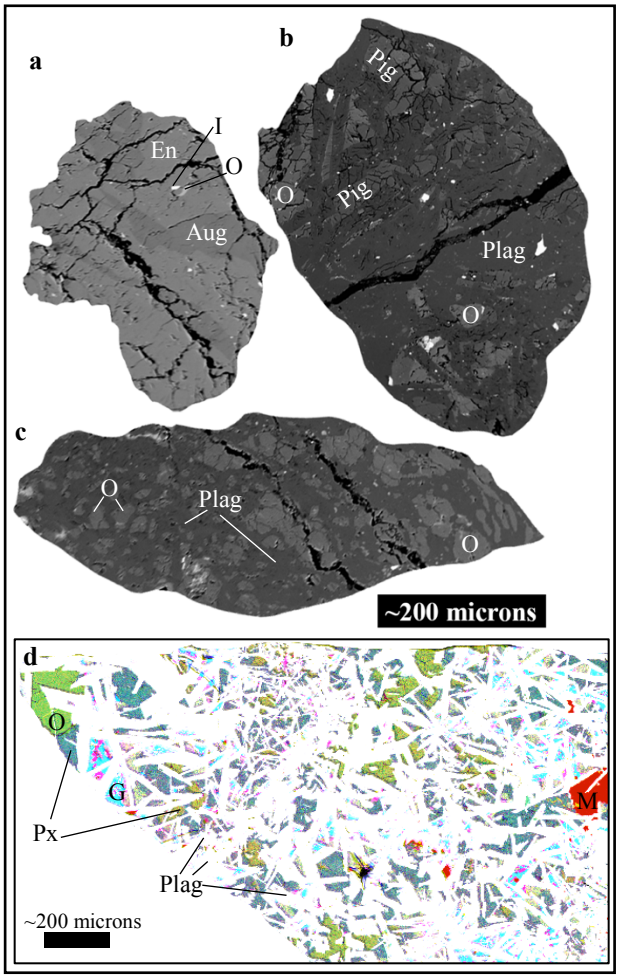

Fig. 1. Representative images of the main clast types; (a)-(c) are backscattered electron (BSE) images, and (d) is a composite X-ray map. Example mineral phases are identified as O (olivine), En (enstatite), Aug (augite), Pig (pigeonite), Px (pyroxene), I (ilmenite), M (Fe-Ni metal), and G (K-rich glass). (a) Clast 1, (b) Clast 2, (c) Clast 6. (d) Clast 7 (Ti-pink, Al-white, Ca-yellow, Fe-red, K-cyan, Si-blue, Mg-green).

Ages: ^{40}Ar-^{39}Ar age determinations were performed using stepped laser heating of two subsplits of NWA 8783- 'dark' (1.81 mg mass removed from dark glassy matrix) and 'light' (2.04 mg mass removed from a light-colored clast coordinating with Clast 7, Fig 1d). Samples were irradiated at the Safari reactor in South Africa. Aliquots of Hb3gr monitor (1074.9 ± 3.5 Ma; [10]) were positioned within a few mm to the samples, which were irradiated in silica glass vials. The J value, a parameter that is representative of the neutron irradiation conditions, was 0.0113915 ± 0.0001124 (1σ) (0.98%).

Stepped heating was performed using a Photon Machines Fusions IR 10.6 µm wavelength CO_2 laser coupled to a Thermo Scientific™ Argus VI preparation bench and multi-collector mass spectrometer at the University of Manchester. Samples were lasered using a 3 mm defocused beam for 30-60s with increasing output power at each step until the sample was degassed. Released gas was cleaned for 2 min on a hot getter, and then 1 min on a hot and cold getter prior to introduction to the mass spectrometer. Isotopes were measured simultaneously and in peak jumping mode: ^{40}Ar, ^{39}Ar, ^{38}Ar, ^{37}Ar and ^{36}Ar were measured on Faraday cups. Data have been corrected for blank contribution, mass discrimination, neutron-induced interference isotope production on ^{40}Ar, ^{39}Ar, ^{38}Ar, and ^{36}Ar and decay of ^{37}Ar and ^{39}Ar and using the decay constants of [11].

Results and Discussion: *Mineral Geochemistry:* Mineral compositional ranges are reported in Table 1 and Figs. 2 and 3. The Mg# of the mafic phases and An content of plagioclase can distinguish between members of the Mg-suite and the FANs (Fig. 2). Clasts 2, 3, and 6 lie within the Mg-suite range [13, 14]; in addition, the pyroxene end-member compositions of Clast 3 (Fig. 3) are similar to Mg-suite pyroxenes [e.g., 15 and refs therein]. Depending on the field limits for the Mg-suite (e.g., [13] vs. [14]), Clast 5 may lie between the fields for the Mg-suite and FAN, which could indicate that this clast represents a Magnesian Anorthosite (MAN). Clast 1 lacks plagioclase and therefore cannot use An% for classification, but the pyroxene compositions are consistent with that of a FAN [e.g. 15 and refs therein].

The modal mineralogy, texture, and mineral phase chemistry of Clast 7 is similar to several Apollo 16 impact melts [e.g., 16], and implies a similar history.

Table 1. Selected summary Compositional Data

Clast #	Fo (N)	Px (N)	An (N)	Px Mg#	$Mg\#_{avg}$ Mafic Phases
1	50 (1)	A (6)	-	72-75	66
		E (6)		61-62	
2	73-77 (7)	P (10)	90-93 (7)	77-79	77
3	70-71 (6)	A (1)	91-92 (3)	79	76
		P (1)		75	
		E (7)		76-86	
5	72-73 (5)	A (2)	95-96 (6)	77-78	74
		P (4)		73-34	
6	78-82 (6)	-	92-96 (5)		81
7	68-76 (7)	A (4)	90-92 (7)	76-78	75
		P (12)		69-78	

Age Dates: The 'light' clast (i.e., the impact melt clast), which has no solar wind component, does not produce a clear plateau and is disturbed, but a weighted mean of the high temperature steps is 3479±29 Ma (2σ) (95% conf. MSWD = 2.0). This likely represents a minimum age of resetting and may indicate a disturbance after the initial crystallization of the impact melt. In contrast, the 'dark' aliquot has a large solar wind component and therefore represents the regolith; the age spectra is highly disturbed and produces no plateau, but Ar data will be used to determine the closure age.

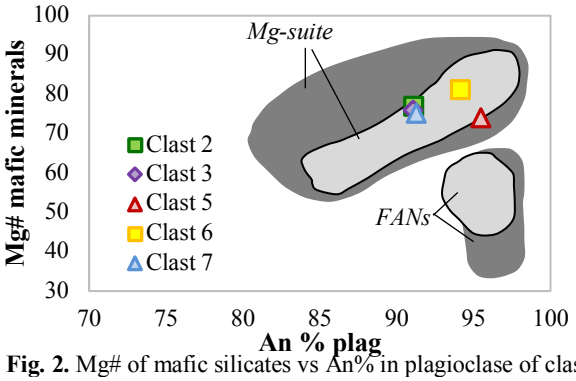

Fig. 2. Mg# of mafic silicates vs An% in plagioclase of clasts in NWA 8783 compared to Mg-suite and FAN fields of [13] (light grey) vs. [15] (dark grey)

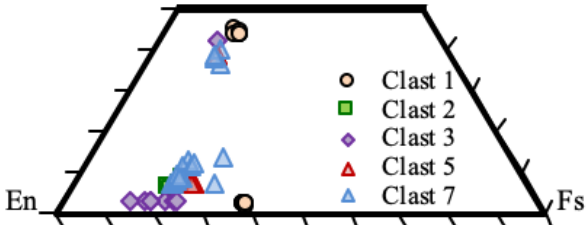

Fig. 3. Pyroxene compositions of clasts in NWA8783.

Implications: NWA 8783 provides information about the bombardment history and lithic diversity of the lunar surface. For example, the impact melt clast (Clast 7, 'light' clast) is similar (texture and mineral chemistry) to several of the Apollo 16 samples [16], which suggests a similar target material, although there is an age difference. In addition, there has been an increasing interest in the role of the Mg-suite and MAN samples, therefore a more detailed examination of the clasts within this sample may yield important findings of the crystallization and evolution of the lunar crust.

References: [1] Joy K.H. et al. (2012) *Science*, **336**, 1426-1429. [2] Fagan A.L. et al. (2016) *LPSC* **47**, Abs# 2789. [3] Robinson K.L. et al. (2018) *LPSC* **49**, 1454. [4] Morris R.V. et al. (1978) *LPSC* **9**, 2033-2048. [5] National Research Council (2007) *Sci. Context. Expl. Moon*, http://www.nap.edu/catalog/11954.html. [6] Lunar Exploration Roadmap (v.2016) https://www.lpi.usra.edu/leag/LER-2016.pdf. [7] LEAG Special Action Team (2018) *Adv. Sci. of the Moon.*, https://www.lpi.usra.edu/leag/reports/ASM-SAT-Report-final.pdf. [8] Korotev R.L. & Irving A.J. (2015) *LPSC* 46, Abst. #1942. [9] Korotev R.L. & Irving A.J. (2016) *LPSC* 47, Abst. #1358. [10] Schwarz, W.H. & Trieloff, M., 2007. *Chem. Geol.*, **242**, 218-231. [11] Renee P.A. et al. (2010) *GCA* **74**, 5349-5367. [12] Lofgren G.E. (1977) *Proc. LSC.*, 2079-2095. [13] Takeda H. et al. (2006) *EPSL.*, **247**, 171-184. [14] Shearer C.K. et al. (2015) *Am. Mineral.*, **100**, 294-325. [15] Curran N. (2017) *PhD Thesis.* [16] Neal C.R. & Fagan A.L. (2012) *LPSC*, **43**, Abs# 2248.